Wood Sci Technol (2014) 48:855–871
DOI 10.1007/s00226-014-0645-0

ORIGINAL

Linear friction welding of spruce boards: experimental investigations on scale effects due to humidity evaporation

Benjamin Hahn · Bernhard Stamm · Yves Weinand

Received: 30 January 2014 / Published online: 5 June 2014

Abstract Recent investigations on friction-welded wood-to-wood connections have shown interesting capacities of these adhesive-free joints for further development towards constructional elements. This paper addresses challenges and technical requirements for the enhancement of this technology from small specimens to samples of structural scale. Inhomogeneities in bonding quality and joint strength, herein referred to as scale effects, become relevant with an increase in size of the welded interface. It is assumed that the water vapour and smoke that evolves during the welding process by evaporation of moisture within the cell structure is a reason for these inhomogeneities. In order to achieve a better understanding of these effects, the influence of the water vapour on welded spruce (*Picea abies*) boards was investigated. It was shown that the vapour increases the internal gas pressure within the welding zone. Thus, it strongly influences the welding process and the quality of the joint. The results of these investigations lead to technical solutions, permitting a significant attenuation of the negative effects and improvement in quality and joint resistance.

Introduction

Friction welding of wood

Welding of wood is an adhesive-free bonding technology based on friction welding technologies as used for thermoplastic materials and metals. In order to achieve a laminar wood-to-wood connection, the interface between two timber boards is heated by a fast and short oscillating frictional movement combined with pressure.

B. Hahn (✉) · B. Stamm · Y. Weinand
Laboratory for Timber Construction IBOIS, EPFL Lausanne, Lausanne, Switzerland
e-mail: Benjamin.Hahn@epfl.ch

The thermal energy, which is evolved, generates high temperatures of up to 440 °C (Stamm et al. 2005a), which lead to a thermal decomposition of the polymeric compounds in the wood cell material, such as cellulose, hemicelluloses and especially lignin (Stamm et al. 2006). The thermo-chemical degradation process taking place during friction welding is referred to as pyrolysis, describing a thermal decomposition of biomass (or organic material) in the absence of oxygen into solids (charcoal), liquids (tar, pitch) and gaseous products (Maschio et al. 1992). Here, the products of this degradation process form a viscous layer of thermally softened material, which hardens when the friction movement is stopped and the interface is cooling down, while a certain cooling pressure is applied. Additionally, a huge amount of smoke gas is generated and ejected from the interface. The following process parameters can be defined: frequency, amplitude, welding pressure and welding time or welding displacement as control values. The latter stands for thickness loss due to decomposition of material close to the contact area. Besides the mentioned machine settings, anatomical parameters related to the characteristics of the welded wood, such as wood species, density, annual ring orientation, moisture content and sample size have important effects on the resulting bond quality (Properzi et al. 2005; Omrani et al. 2010). Research at the Laboratory for Timber Construction IBOIS at the EPFL focuses on two principal wood types that are commonly used for timber construction, spruce as a representative for softwood and beech for hardwood. Shear bond strengths that can be achieved with these two types of wood are 3.5 MPa for spruce (Placencia et al. 2011) and 13.4 MPa for beech (Mansouri et al. 2009). Stamm et al. (2011) showed that especially the moisture content of spruce samples strongly influences the shear resistance of the welded connection. It could be shown that a reduction in the moisture content led to higher joint strength and smaller standard deviation.

Scale effects

First investigations on welded timber joints were limited to small surfaces of around 3,000 mm^2 (Stamm et al. 2005a, 2006; Properzi et al. 2005; Omrani et al. 2010) due to mechanical limitations of the welding devices. Welding of bigger surfaces up to 50,000 mm^2 became possible in 2006 with the construction of a new welding installation that was specially conceived for wood. Visual evaluations have shown that the welding process, developed on small size specimens, cannot be applied in the same way to larger surfaces. For several wood species, especially soft wood, welding did not occur homogeneously over the whole surface. Important central parts of the interface did not show a good weld, while the borders were flawlessly welded. This is due to the lack of a significant thermal change of the cell material at the position where these effects occur. Previous tests at the IBOIS showed that these effects disappeared for welding of samples with a reduced moisture content of 4 %.

It is assumed that the evaporation of moisture, bound within the cell structure of the wood matrix and emitted together with volatiles of the thermally decomposed wood material during welding (Omrani et al. 2008), leads to an internal gas pressure within the interface. With increasing surface size A, the amount of evaporated moisture increases correspondingly, while the length U of the slit at the edges,

through which the vapour can escape, rises at a lower rate than A. Equation 1 illustrates this relation for quadratic surfaces. Consequently, the internal gas pressure increases. This pressure is suspected to reduce the friction between the contact surfaces and hence as well the generation of frictional heat, necessary to gain a weld. Provided that the assumption is right, a reduction in the internal gas pressure should lead to a more homogeneous welding quality of the joint.

$$\frac{A_2}{A_1} = \left(\frac{U_2}{U_1}\right)^2 \tag{1}$$

Objectives

Experimental investigations were carried out in order to understand the reasons for the occurrence of scale effects and to demonstrate their influence on the welding result. For further development of this technology towards industrial fabrication of constructive components, these effects have to be prevented. Specimens were modified in order to reduce the internal gas pressure, produced by a large smoke generation during welding. The effects of these modifications on specific process parameters, such as interface temperature and gas pressure, and the distribution of the interfacial shear resistance at different points of the interface were analysed. The observed results are used for defining technical measures, adapted to reduce these scale effects.

Experimental investigations

The experimental investigations deal with the influence of the reduction in the internal gas pressure through different modifications of the specimens on the quality of the welding result. It is assumed that the internal gas pressure can be decreased by facilitating the transport of the vapour from the interface to the outside through gas evacuation channels at the contact surface. Another possibility is to decrease the amount of water vapour within the generated gas mixture, evaporated from the cell structure during the heating of the wood samples, by reducing the moisture content. For the investigations, in addition to the normal surface conditions, three sample modifications have been established. The details of these modifications are listed in Table 1. The relationship between the internal gas pressure and the resulting bond quality was examined by means of three different test set-ups. The conceptual approaches of these investigations are described in the following, while the test procedures themselves are explained in "Gas pressure measurements, Shear strength distribution and Temperature measurements sections".

A measuring device was developed in order to detect the internal gas pressure, generated at the interface, at different positions during welding. A modification of the welded surface by the use of channels carved into the surface or by a reduction in the moisture content should significantly decrease the gas pressure measured. The detected signal allows for comparison between the welding pressure applied on the outside of the specimen by the welding machine and the internal gas pressure.

Table 1 Sets of specimen surface conditions for experimental investigations

	Moisture content (MC) (%)	Surface grooves	
Set A	11.3	None	(Fig. 1a)
Set B	3.9	None	(Fig. 1a)
Set C	11.3	Longitudinal surface grooves	(Fig. 1b)
Set D	11.3	Perpendicular surface grooves	(Fig. 1c)

Local detracting of the welding process provoked by the internal gas pressure has an influence on the welding quality and the homogeneity of the resulting joint strength over the surface. The set-up of a shear strength distribution profile, where strength values are estimated at different positions of the bonded surface, was carried out. With the reduction of the internal gas pressure, the strength distribution should be homogenised.

Previous temperature measurements at the interface during friction welding have shown a characteristic progression of heat evolution during the process (Stamm et al. 2005b). Since the heat generation rate is directly correlated with the coefficient of friction, the aforementioned reduction in the latter due to the internal gas pressure must be detectable in form of a decrease in heat generation at the centre of the heated zone. At the same time, a reduction in the internal gas pressure should lead to a more homogeneous evolution of all temperature curves at different positions of the interface. In order to prove this, a set of thermocouples was arranged at different positions of the contact area before welding. A comparison between temperature curves and visual evaluation for different surface conditions allows for a conclusion of the influence of the vapour generation on the heat generation during the welding process.

Material

High-quality knot-free spruce wood (*Picea abies*) was used for the investigations. In order to gain significant results, a strict selection of the timber boards is necessary to allow for a reduction in the natural scattering of the material due to inherent anatomical variations. The wood was conditioned in two manners according to the specimen conditions in Table 1: (a) one part was stored at 20 °C and 65 % RH relative air humidity. Measurements showed a moisture content MC of 11.3 %. (b) In order to reduce the amount of evaporated moisture in the evaporated gas mixture during welding, another part of the samples was stored in a climate oven calibrated to 40 °C and 27 % RH and dried to a moisture content of 3.9 %. Foregoing tests on friction-welded double lap joints (Hahn et al. 2012) stored under the same conditions showed very good homogeneity of the interface and lower scattering of the measured shear strength.

Specimens' description

For all investigations, four types of specimens can be distinguished according to Table 1. Set A represents the reference conditions where scale effects have

previously been observed. This set of specimens had a moisture content of 11.3 % and a plane-welding zone without additional surface grooves for smoke evacuation. The same applies to set B for which the moisture content was reduced to 3.9 % in order to decrease the amount of evaporated moisture within the gas mixture. To improve the smoke transport from the interface to the edges during welding, longitudinal and perpendicular grooves were arranged in the surface of the contact area of specimens from set C and D. Figure 1 shows the modifications of the specimens before welding.

The geometry of the welded timber parts changed according to the type of investigations. Gas pressure measurement was carried out on samples with a quadratic contact area of 160 × 160 mm^2. In order to be able to install the pressure sensor, one of the welded elements had a thickness of 45 mm, while the opposite part was 20 mm thick. The test set-up is described in "Gas pressure measurements" section.

For the investigations on heat generation and the estimation of the shear strength profile, timber boards with dimensions of 320 × 100 mm^2 were welded. These dimensions correspond to geometries where scale effects have been observed initially. The test set-up for the determination of a shear strength distribution after welding is described in "Shear strength distribution" section, while "Temperature measurements" section describes the temperature measurements during welding.

The welding parameters, listed below at the end of each description of the test set-ups, are adapted to the investigations and sample geometries and are defined according to empirical values from previous studies (Stamm et al. 2011; Hahn et al. 2012).

Gas pressure measurements

Two gas pressure sensors were placed at two different positions of the interface in order to compare the pressure at the geometrical centre to the pressure at the edge of the interface. Figure 2 shows the dimensions of the specimens, the position of the measuring points and the position of the surface grooves for set C and D. Sensors of the type PX73-100GV (Omega®, Stamford CT/USA) were used. The membrane of the sensors is very sensitive to mechanical impacts and had to be placed outside of

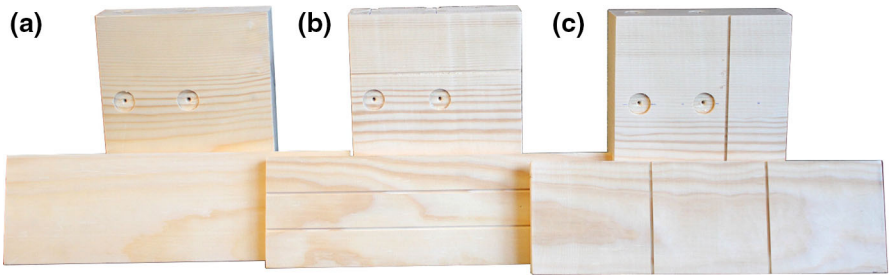

Fig. 1 Spruce samples prepared for the experimental investigations on gas pressure measurements (behind) and temperature and shear strength distribution (front) with different surface conditions: without (**a**), with longitudinal (**b**) and with perpendicular (**c**) gas evacuation channels

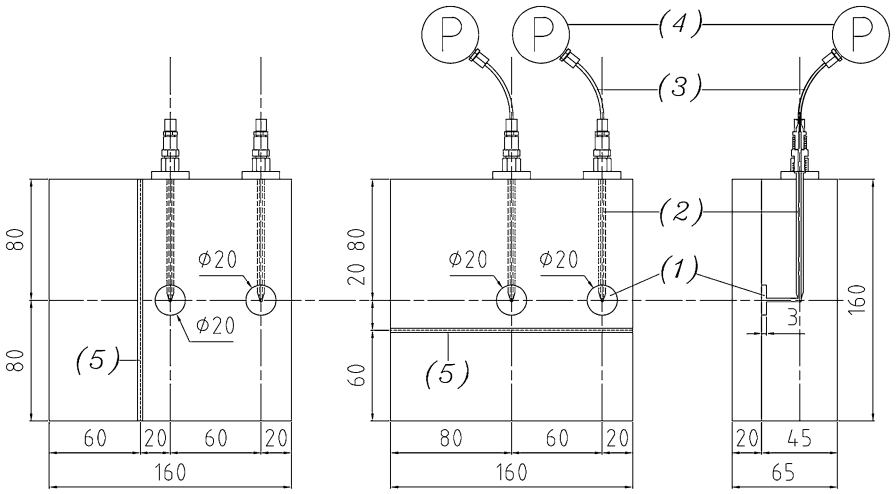

Fig. 2 Test set-up for gas pressure measurements, indicating the void (*1*), metal tube (*2*), elastic pipe (*3*) and the pressure sensor (*4*) as well as the position of the gas evacuation channels (*5*)

the specimen in order to protect it from vibrations occurring during welding. Therefore, a 75-mm-long metal tube was introduced into the thicker part of the sample and connected to the welded interface through a thin hole. From the outer end, a flexible plastic tube transferred the pressure to the sensor, thus preventing the transmission of vibrations from the welding installation to the membrane. The cylindrical void at the interface in Fig. 2 is added in order to prevent the viscous decomposed material from clogging the connection to the metal tube.

For better comparison between the measurements, the welding time t_w was fixed at 6 s. The frictional movement was adjusted to a frequency f of 130 Hz and an amplitude a of 1.5 mm; meanwhile, a welding pressure P_w of 1.1 MPa was applied to the samples. When the welding time t_w was achieved, a cooling pressure P_c of 2.0 MPa was maintained during 30 s. Five samples were welded for each set from Table 1.

Shear strength distribution

The interface of the welded samples of 320 × 100 mm^2 was divided into nine subareas according to Fig. 3. From each subarea small specimens of 100 × 25 × 20 mm^3 were carefully cut out after welding. Subsequently, the samples were prepared for testing according to Fig. 4. A tensile load was applied at the two ends, introducing a shear stress at the interface between the two cuts, until failure occurred. The displacement of the testing device was set to 2 mm/min. From each set of different surface conditions in Table 1, ten samples were tested for each subarea. The average values from each subarea were compiled into four shear strength distribution profiles corresponding to one set of surface condition.

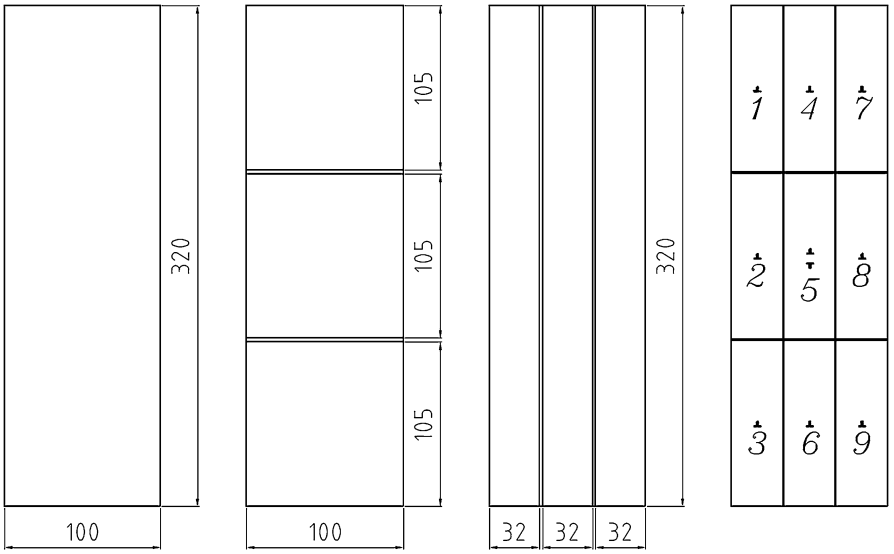

Fig. 3 Dimensions of the spruce boards used for temperature measurements and evaluation of strength distribution including the position of the thermocouples within the subareas (*right*)

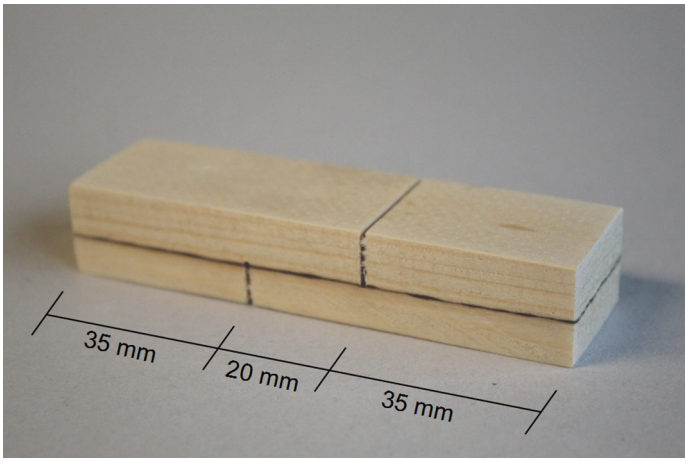

Fig. 4 Small specimen cut out from bigger samples (see Fig. 3) for estimation of the strength distribution profile

For the welding process, the same frequency f, amplitude a and cooling pressure P_c as stated in "Gas pressure measurements" section were used. Contrary to the investigations on gas pressure measurements, the welding pressure P_w was maintained at 1.5 MPa. In order to obtain a welded interface of homogeneous thickness, which is a function of the amount of decomposed cell structure, the

welding displacement d_w was used as criteria instead of the welding time. Here, the friction movement stopped after a welding displacement of 2.0 mm.

Temperature measurements

For temperature measurements, thermocouples of the type K (Ni-CrNi, 2×0.35 mm^2, insulated by glass silk, with a maximum capacity of T_{max} 1,000 °C) were used. One thermocouple was placed in the centre of each subarea from Fig. 3, except for subarea 5, where two elements were used in case that one is damaged during welding. Signals that indicated a defective element were not taken into account. In order to prevent friction between the wood surface and thermocouples, the twisted wires of the thermocouples were embedded in small notches. The cables were conducted orthogonally through one of the welded components. Subsequently, the holes were closed with small wooden sticks combined with glue in order to prevent any escape of the vapour and smoke through these holes.

For each set of surface conditions from Table 1, five samples were welded. The same welding parameters as for gas pressure measurements described in "Gas pressure measurements" section were used for the temperature measurements. The results should also be compared to the results from the strength distribution tests mentioned above.

Results and discussion

Gas pressure measurements

Figure 5 displays the mean values and standard deviations for the measured gas pressures according to different surface conditions described in Table 1. With progressing welding time, the gas pressure at both measurement points increases up to a maximum value at the end of the welding process. The diagrams (a)–(c) show that a much higher pressure occurs at the centre of the square section compared with the measurement point at the edge. For all four test series, the pressure detected at the edge converges towards a value between 1 and 1.2 bar at the end of the welding process. For non-dried samples, the highest ratios between the pressure values at the centre and the edge were observed for set A. Here, the mean internal value of 2.70 bar was almost three times higher than at the edge. This internal pressure value corresponds to approximately 25 % of the external welding pressure applied by the machine onto the sample. Set C had the greatest variation in results. The ratio of internal pressure to edge pressure varied between 4.84 and 1.14, at an average of 2.27. Only when vertical gas evacuation channels in the interface were used in set D, the internal pressure could be significantly reduced to a value close to the pressure at the edge. Here, the average internal pressure of 1.25 bar corresponds to 50 % of the mean value from set A.

It was remarkable that, compared to set A, even in relatively dry samples with about 4 % of moisture content in set B, a high internal pressure of around 3.21 bar

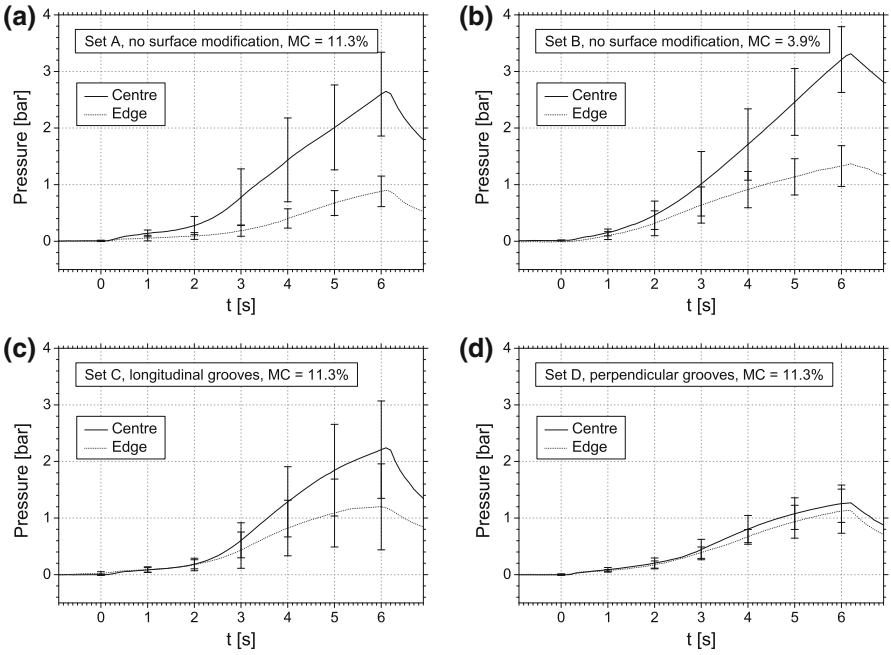

Fig. 5 Mean values and standard deviation of gas pressure measurement for different sets of surface conditions

was measured. On average, the pressure level measured at the end of the welding process at the centre was about 2.56 times higher than at the edge. The fact that the internal pressure is even higher than for set A contradicts the assumption that the internal gas pressure is primarily related to the evaporating moisture in the wood. Numerous investigations showed that chemical reactions involved in pyrolysis processes are rather complex and strongly dependent on various parameters such as temperature (Horne and Williams 1996; Williams and Besler 1996), particle size (Figueiredo et al. 1989; Seebauer et al. 1997), gas pressure (Cetin et al. 2005; Price and Wenger 1992) and moisture content (Demirbas 2004; Guillen and Ibargoitia 1999). The fractions of solid, liquid and gaseous compounds vary according to the chemical and physical conditions (Grønli and Melaaen 2000; Inguanzo et al. 2002). The latter argues that an increase in heating time and heat flux leads to a higher proportion of noncondensable gases. From temperature measurements carried out by Stamm et al. (2005c), it could be concluded that a reduction in moisture content leads to a faster and higher rise in temperature. At the same time, a decrease in moisture content is supposed to lead to an increased proportion of liquid smoke (the part of the smoke that fluidifies when cooling down in a condenser), including certain gaseous components such as phenol, formaldehyde and acids (Guillen and Ibargoitia 1999). Former research at the IBOIS also showed that welding of dry wood runs much faster (Stamm et al. 2011). Here, welding time was fixed at 6 s for all configurations, which means that for rather dry samples of set B more material is

decomposed at the end of the process than for samples with a moisture content of 12 %. This leads to a bigger amount of gaseous products from the pyrolytic decomposition. Besides, no occurrence of scale effects implies that more surface material undergoes pyrolysis processes, and thus, more volatiles are generated. Therefore, the higher value of gas pressure for dry samples can be explained by a combination of these factors: higher temperature, higher heat flux, lower moisture content and a larger amount of decomposed material.

It has to be noted that the measured values are highly influenced by the relatively large volume, composed of the void at the interface and the channels, transmitting the pressure towards the sensor, on the one hand, and the strong and fast heating of the gas mixture on the other hand. When smoke and water vapour are generated at the interface, the void and the channels are filled up before the correct pressure is measured. At the same time, this volume is reduced due to the welding displacement and important quantities of decomposed material from the pyrolysis filling up the void. The results should be regarded as qualitative information rather than quantitative values. Nevertheless, they provide interesting information about the range of the internal pressure, and how it can be influenced.

Shear strength distribution

The resulting shear strength distributions are presented for each set of surface conditions in Fig. 6. Each position of the grid surface represents the mean value of a subsurface from Fig. 3. Set A shows a clear reduction in the mechanical strength towards the centre of the interface. An overall shear resistance of 2.73 MPa for all subareas with a standard deviation of 0.55 MPa corresponding to 20 % was obtained. The mean shear resistance at the centre is reduced to less than 50 % of the value at the corner, which sheds light on the occurring scale effects.

The establishment of gas evacuation grooves at the welded interfaces of specimens with the same moisture content led to a significant reduction in these effects. For example, the shear strength profile for set C with longitudinal smoke evacuation channels is much more homogeneous. With 2.74 MPa, the mean shear resistance for the whole surface was nearly the same as for set A, but the significant reduction in the local results towards the centre disappeared clearly. Instead of a cone in the grid surface at subarea 5, the local shear strength shows the lowest value at subarea 3 with 2.23 MPa, still 0.90 MPa higher than the lowest value of set A. The standard deviation could be reduced to 12 % through this modification of the surface conditions. If perpendicular grooves were used, as it is the case for set D, the overall shear resistance could even be increased up to 3.31 MPa with only a slight drop at the centre of the grid. The standard deviation of 13 % was lower than that of set A. Perpendicular surface grooves seem to be most advantageous since the shear strength results are much higher and more homogeneous than for other surface conditions of samples with the same moisture content of 11.3 %. The reduction in the moisture content to 3.9 % in set B led to the highest overall mean shear strength of all four sets of surface conditions. The mean of all nine subareas scattered around 3.5 MPa with a standard deviation of 8 %, with slightly decreased values towards the centre.

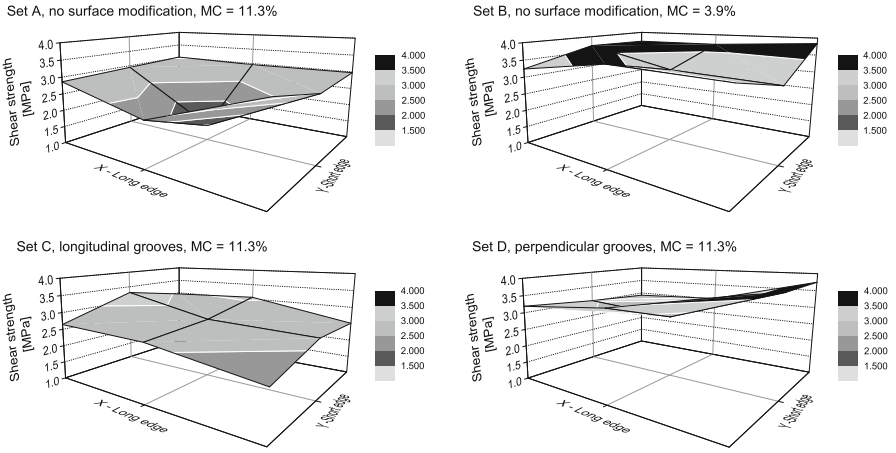

Fig. 6 Shear strength distribution profiles for different surface conditions. Each point of the grid surface corresponds to the average shear strength of ten small samples (Fig. 4) cut out at the position of each subarea (Fig. 3)

However, this approach of using reduced moisture content is not suitable for practical use. On the one hand, an increased amount of energy is required for the preparation of the timber. On the other hand, this method includes a large difference between initial moisture content and the moisture content during application, here approximately 12 % for internal use. The latter is a huge disadvantage, since swelling and shrinking deformations occur due to the resulting increase in moisture, provoking cracks in the welded joint and leading to failure of the corresponding component. Therefore, it is more adequate to weld the wood with a moisture content that corresponds to the conditions of the subsequent application.

Temperature measurements

Visual evaluations

The samples were opened after welding in order to evaluate the welding result visually. The opened samples are shown in Fig. 7. Scale effects can be observed in the interface of the samples from set A. Large bright areas where insufficient welding occurred are clearly visible. A reduction in the moisture content to 3.9 % in set B results in a more homogeneously welded surface area. Nevertheless, small areas still remain hardly thermally decomposed. Longitudinal surface grooves of set C could reduce the scale effects as well if the moisture content was kept at 11.3 %, even if significant areas remain insufficiently welded. For the same moisture content, the best visual homogeneity occurred for samples with perpendicular surface grooves in the welded interface. The bright spots in sample TD02 result from wood fibres that remained attached to the opposite piece of wood. Visually, perpendicular surface grooves seem to be most appropriate to

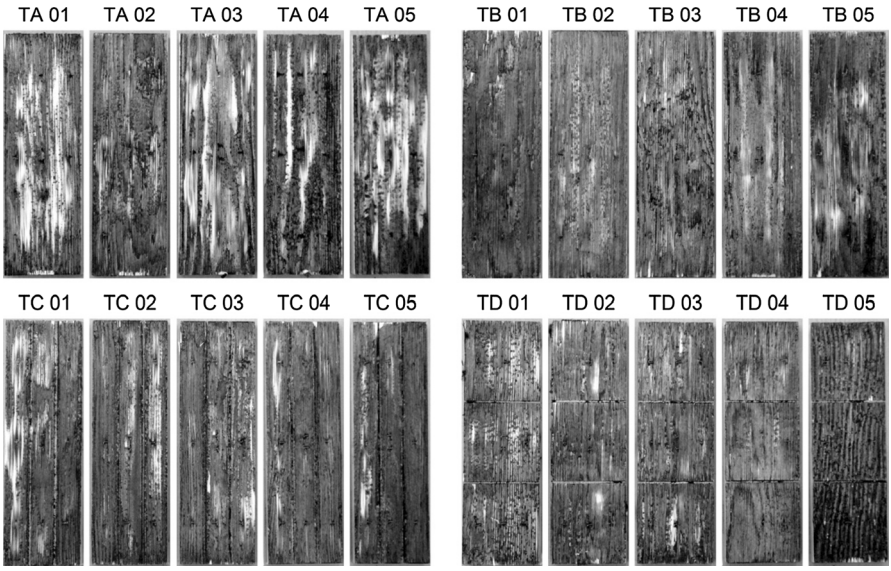

Fig. 7 Visual evaluation of the opened samples after welding. The bright areas within the darkened and thermally modified bond material illustrate the occurrence of local scale effects within the welded interface

avoid the appearance of scale effects if spruce boards with a standard amount of moisture of around 12 % are welded.

Distribution of the temperature at the interface

After visual evaluation, the results from interfacial temperature measurement of each specimen were compared to the corresponding image of the welded interface from Fig. 7. For the graphical illustration, the particular signals from each thermocouple were classified into four distinct groups, representing each one type of subarea *Centre*, *Corner*, *Long edge* and *Short edge*. The temperature curves for three most distinct cases TA01, TA03 and TA04, where scale effects occurred most clearly, are given in Fig. 8. An evaluation of the measurements from TA05 was neglected because of the damage of three thermocouples. In all cases, the temperature increases continuously during the friction phase and converges to a maximum value of around 350 °C at $t_W = 6$ s. Interest is focussed mainly on the temperature at the centre of the interface where scale effects are expected to occur.

For the given examples of sample TA01, TA03 and TA04, the distribution of the temperature curves shows three completely different characteristics. A correlation between the temperature values and the visual quality of the bond cannot be observed. Furthermore, no specific differences in the measurements of set B to D are observed. The measurement curves reached similar values and similar distributions for all sets as in the graphs in Fig. 8, although visually much better welding results were obtained. No correlation between the surface conditions from Table 1 and the

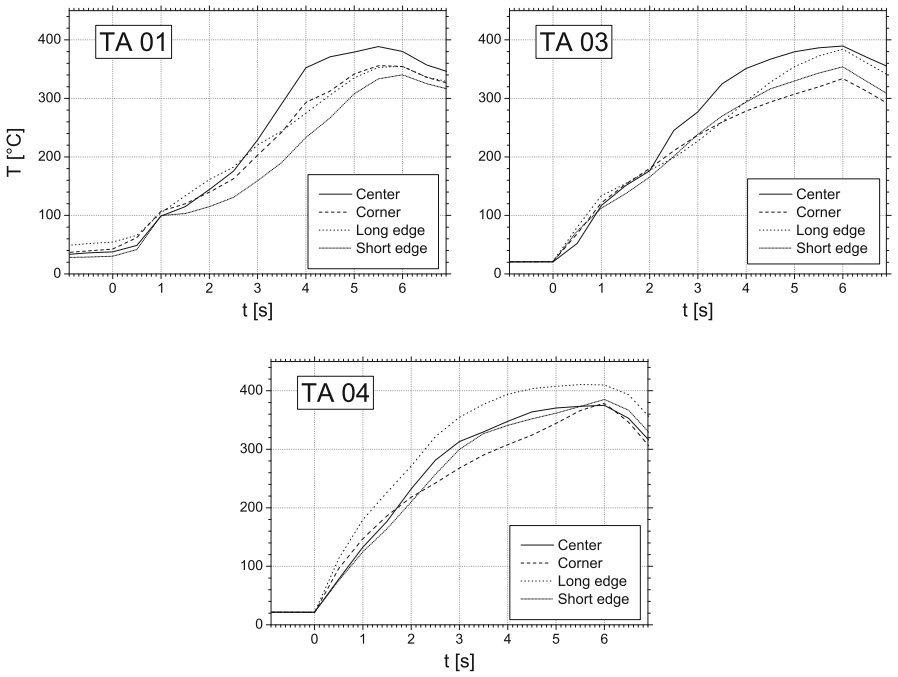

Fig. 8 Temperature curves for selected samples from set A. The different drawing of the curves corresponds to four predefined groups of subareas (see Fig. 3), namely *centre* (subarea 5), *corner* (1, 3, 7 and 9), *long edge* (2 and 8) and *short edge* (4 and 6). The average value is represented in the graphs

temperature, as it was the case for the shear strength distribution, could be observed. For the sake of clarity, it was decided not to show these results here. However, it can be observed that the opened interfaces in Fig. 7 show locally darkened, and thus thermally modified, spots within the bright and barely welded zone. These discontinuities occur exactly at the positions where the thermocouples have been placed, namely in the case of TA01, TA03 and TC01. It is possible that the grid of measuring points was not tight enough to clearly detect zones where heat generation is disturbed or retarded. Another possibility is that the thermocouples themselves represent a certain local discontinuity within the welded interface where higher temperatures are reached, even if scale effects occur in the surroundings. In these cases, scale effects cannot be related to the temperature curves.

Complementary measurements

It was decided to verify these assumptions through a new set of tests using a denser distribution of the measuring points. Samples with identical dimensions and a moisture content of 12 % were welded. Twelve thermocouples along two lines were arranged transversely to the longitudinal direction (see Fig. 9). One line of thermocouples was arranged 10 mm from the edge, and the second line was placed at the transversal axis of symmetry at 160 mm. The same welding parameters as

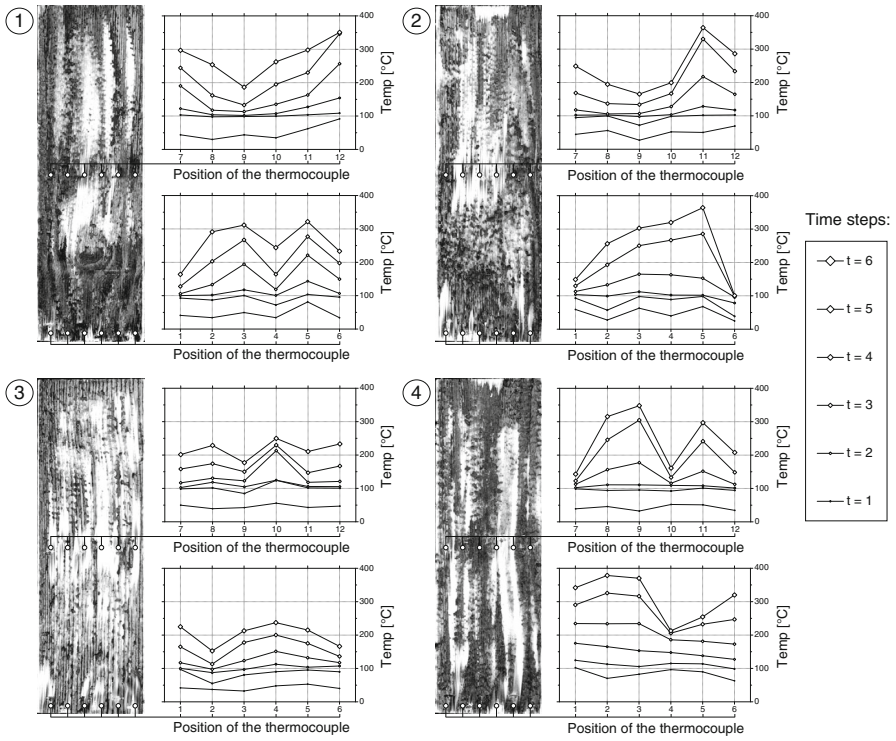

Fig. 9 Temperature curves resulting from complementary measurements at different time steps $t = 1$ s to $t = 6$ s. The first line of thermocouples close to the edge corresponds to the position 1–6, while the measuring points in the centre of the interface correspond to position 7–12

defined in "Gas pressure measurements" section were used. The open interface of four representative specimens is shown in Fig. 9. For each sample, the temperature values at the different positions at different time steps are given.

Scale effects occur in the same manner as in the samples of set A. All temperature graphs show a decelerated rise in temperature between $t = 2$ s and 3 s at around 100 °C, the temperature where water evaporates from the cell structure. The zones at which scale effects occur can be associated with positions of the lowest temperatures in the graphs (generally below 200 °C), where further temperature increase is retarded. The long bright area in sample 1 is reflected by a decrease in temperature towards position 9. The edge is well welded except a small bright area at position 1 where low temperature values occurred. Sample 2 also has a large bright area in the centre, which can be compared to the low temperature values at positions 8–10. The interface of sample 3 is generally less degraded, which can be confirmed by the overall low temperatures. The long conspicuous bright area from sample 4, which has a slight offset to the right of the longitudinal axis, can be related to the low temperature both in the centre (pos. 10) as well as at the edge (pos. 4). The new graphs show a good correlation with the visual results. Local discontinuities are represented by the deceleration in increasing temperature at the

locations of less degraded interface zones, even if they occur close to the edge. The results prove that scale effects can be associated with a reduced heat generation during friction, leading to insufficiently welded bonds.

Conclusion

To shed light on the occurrence of scale effects, consisting of significant inhomogeneities in bond quality during friction welding of wood samples with larger surface areas, different experimental approaches have been conducted. The results allowed for the following conclusions:

1. Temperature measurements clearly showed that the occurrence of scale effects goes along with a decelerated increase in temperature during the welding process at the positions where they occur.
2. During friction welding, an important gas pressure is generated at the centre of the interface. This gas pressure results not only from the evaporation of moisture from the wood but also from the release of an important amount of volatiles due to the thermal degradation process taking place during welding (Stamm et al. 2006; Omrani et al. 2008). By facilitating smoke transport from the interface by gas evacuation channels perpendicular to the grain, the internal pressure could be reduced to a value similar to the pressure measured close to the edge that was similar for all specimen variations.
3. For samples with moisture content of 11.3 %, a reduction in the internal gas pressure by means of gas evacuation channels influences the occurrence of scale effects. Visual evaluations of the interface quality after welding as well as mechanical shear strength estimations showed that inhomogeneities in bond quality could significantly be reduced especially when channels perpendicular to the grain were used.
4. The moisture content of the wood samples is not, as it was assumed, positively related to the internal gas pressure. Reduced moisture content does not necessarily lead to a reduction in the internal smoke gas pressure. However, it leads to a significant reduction in scale effects and much higher mechanical joint strength. The reason might be that heat energy is consumed for the evaporation of moisture from the cell structure and is not available for the pyrolysis. Therefore, at the positions where evaporation is hindered or decelerated, thermal degradation is retarded, and scale effects occur.
5. The investigations could clearly prove the existence and the effects of an internal gas pressure caused by the smoke generation from the thermal degradation process during friction welding. Especially the evaporated moisture seems to have an important influence on the welding process, since dry samples with a moisture content of 3.9 % did not show scale effects, but an important amount of internal smoke gas pressure was detected.
6. The experimental results showed that scale effects increase with increasing length of the boards. Through the introduction of perpendicular channels into the contact area, better welding results were obtained for non-dried samples of

11.3 % moisture content. The distribution of the bond strength over the total joint surface showed a much better homogeneity compared with samples without or with longitudinal smoke evacuation channels. The overall average strength still reached 95 % of the strength from samples with low moisture content. Therefore, the use of this modification could be a simple and practical approach that helps to improve joint quality when large samples are welded.

Acknowledgments The present research work is funded by the Swiss National Foundation and is part of the project "SNF-Synergia Project no. CRSI22_127467/1".

References

Cetin E, Guupta R, Moghtaderi B (2005) Effect of pyrolysis pressure and heating rate on radiata pine char structure and apparent gasification reactivity. Fuel 84:1328–1334

Demirbas A (2004) Effect of initial moisture content on the yields of oily products from pyrolysis of biomass. J Anal Appl Pyrolysis 71:803–815

Figueiredo JL, Valenzuela C, Bernalte A, Encinar JM (1989) Pyrolysis of holm-oak wood: influence of temperature and particle size. Fuel 68:1012–1016

Grønli MG, Melaaen MC (2000) Mathematical model for wood pyrolysis—comparison of experimental measurements with model predictions. Energy Fuels 14:791–800

Guillen MD, Ibargoitia ML (1999) Influence of the moisture content on the composition of the liquid smoke produced in the pyrolysis process of *Fagus sylvatica* L. Wood J Agric Food Chem 47:4126–4136

Hahn B, Vallée T, Stamm B, Weinand Y (2012) Experimental investigations and probabilistic strength prediction of linear welded double lap joints composed of timber. Int J Adhes Adhes 39:42–48

Horne PA, Williams PT (1996) Influence of temperature on the products from the flash pyrolysis of biomass. Fuel 75(9):1051–1059

Inguanzo M, Dominguez A, Menendez JA, Blanco CG, Pis JJ (2002) On the pyrolysis of sewage sludge: the influence of pyrolysis conditions on solid, liquid and gas fractions. J Anal Appl Pyrolysis 63:209–222

Mansouri HR, Omrani P, Pizzi A (2009) Improving the water resistance of linear vibration-welded wood joints. J Adhes Sci Technol 23:63–70

Maschio G, Koufopanos C, Lucchesi A (1992) Pyrolysis, a promising route for biomass utilization. Bioresour Technol 42:219–231

Omrani P, Masson E, Pizzi A, Mansouri HR (2008) Emission of gases and degradation volatiles from polymeric wood constituents in friction welding of wood dowels. Polym Degrad Stab 93:794–799

Omrani P, Mansouri HR, Pizzi A, Masson E (2010) Influence of grain direction and pre-heating on linear wood welding. Eur J Wood Prod 68:113–114

Placencia MI, Pizzi A, Pichelin F (2011) Linear friction welding for wood, a parameters study for upscaled assemblies. CIMAD 11–1° Congresso Ibero-Latino Americano de Madeira naConstrução. Coimbra (Portugal)

Price LC, Wenger LM (1992) The influence of pressure on petroleum generation and maturation as suggested by aqueous pyrolysis. Adv Org Geochem 19(1–3):141–159

Properzi M, Leban JM, Pizzi A, Wieland S, Pichelin F, Lehmann M (2005) Influence of grain direction in vibrational wood welding. Holzforschung 59:23–27

Seebauer V, Petek J, Staudinger G (1997) Effects of particle size, heating rate and pressure on measurement of pyrolysis kinetics by thermogravimetric analysis. Fuel 76(13):1277–1282

Stamm B, Natterer J, Navi P (2005a) Joining of wood layers by friction welding. J Adhes Sci Technol 19(13–14):1129–1139

Stamm B, Natterer J, Navi P (2005b) Joining wood by friction welding. Holz Roh- Werkst 63:313–320

Stamm B, Natterer J, Navi P (2005c) Development of friction welding of wood: physical, mechanical and chemical studies. PhD thesis no. 3396. Ecole Polytechnique Fédérale de Lausanne EPFL

Stamm B, Windeisen E, Natterer J, Wegener G (2006) Chemical Investigations on the thermal behaviour of wood during friction welding. Wood Sci Technol 40:615–627

Stamm B, Weinand Y, Hahn B, Rossmair G (2011) Influence of the moisture content on the shear strength of welded wood-to-wood connections. COST Action FP0904 Thermo-hydro-mechanical wood behaviour and processing, book of abstracts 131–133

Williams PT, Besler S (1996) The influence of temperature and heating rate on the slow pyrolysis of biomass. Renew Energy 3:233–250